ISABE-2005-1143

VALIDATION METHODOLOGY FOR THE DEVELOPMENT OF LOW EMISSION FUEL INJECTORS FOR AERO-ENGINES

C. Hassa*, J. Heinze*, L. Rackwitz°, Th. Doerr°

*DLR – German Aerospace Center, Institute of Propulsion Technology
Linder Höhe, 51147 Cologne, Germany
°Rolls-Royce Deutschland Ltd & Co KG, Eschenweg 11
15827 Blankenfelde-Mahlow/Berlin, Germany

Keywords: *Aeroengine, Combustion, Low emission, Optical measurements, Validation Method*

Abstract

This contribution describes a newly derived development chain for the early design and validation phases of lean burning injectors allowing a faster and cheaper design process. It comprises an initial concept definition, design optimizations based on CFD and a design validation by qualitative fuel flow tests, followed by the application of laser diagnostic methods. Finally, emission and operability characteristics are determined at real operating conditions.

The comprehensiveness of the applied development chain has been proved to significantly reduce NO_x emissions of the lean burners and to generate validated design rules for the fuel injectors analyzed in this study.

Nomenclature

AFR	air-to-fuel-ratio
CFD	computational fluid dynamics
EI	emission index [g /kg fuel]
FFN	fuel flow number, normalized
HPSS	high-pressure-single sector
LIF	Laser induced fluorescence
LPP	lean premixed prevaporized
NOx	oxides of nitrogen (NO, NO2)
P_{air}	inlet pressure, air [bar]
PDA	Phase Doppler anemometry
r	normalized wall distance [%]
SSC	single sector combustor with optical access
T_{air}	inlet temperature, air [K]
μ	pilot fuel split [%]

Subscripts

d	design

1. Introduction

Future aero-engines need to be affordable, highly efficient and environmentally friendly. New regulations on emissions coming into effect in 2008 will demand a further NO_x reduction. Combined with increased pressure ratios and turbine inlet temperatures to improve component efficiencies, significant steps must be taken in combustion technology to achieve emissions with a sufficient margin to the allowed limits.

Lean Combustion is the most promising low emission combustion concept for NOx reduction of aero-engine combustors. The success of lean combustion techniques strongly depends on the homogeneity of the premixing process, which has to be accomplished within the fuel injection device and in its downstream vicinity. An inherent problem of lean combustion is the reduced combustion stability and its margin against weak extinction. Therefore, lean combustors are equipped with piloting devices to retain full combustor operability and the required turn-down ratios for aero-engine applications. This fuel staging can be achieved within radially or axially staged combustor architectures adding significant

complexity and thus penalties for cost and weight onto the combustion system. Another approach for fuel staging is to accomplish the pilot stage within the lean premixing fuel injector. As a consequence both low and high power performance and thus most of the aero-engine combustor requirements are focused on the fuel injector. Beside combustor cooling aspects combustor development is concentrated on fuel injector development. Designing combustors for low emissions, high stability against weak extinction and a low propensity to thermo-acoustic fluctuation requires a detailed understanding of fuel preparation, fuel placement, pilot and main reaction zones and flame interactions. The design and validation methodology for such a fuel injector development is described within this paper comprising principal layout and optimisation by CFD, detailed investigation with non-intrusive laser measurement techniques and validation at nominal operating conditions.

2. Development chain

Due to the high sensitivity of design changes on combustion performance and because of the limited prediction accuracy of numerical methods for lean combustion the development process for modern fuel injectors has to include precise validation steps. In general, numerous design variables exist and a multitude of configurations can be derived for testing, therefore optimization can be arduous task. In the current study, a newly derived development chain for the early design and validation phases of fuel injectors was derived allowing a faster and cheaper design process. **Figure 1** shows the applied development chain for the detailed investigation and optimization of low emission injectors. Within the German E3E project [1] the basic layout of the injector was derived. After the concept definition phase CFD methods were applied to estimate suitable design variants of the basic concept.

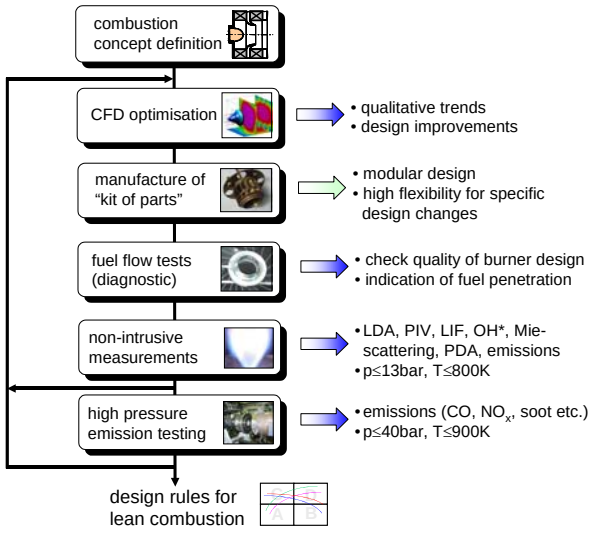

Figure 1 - Applied development chain for the early design phase of lean injectors

In a next step, a set of injector variants was then manufactured. To isolate effects of design changes on burner performance and to allow gradual modifications to the basic design without a high cost penalty, the injector has been designed as a "kit of parts" e.g. all components such as air swirlers and fuel injection devices can be exchanged quite easily.

The first step of experimental validation was to carry out fuel flow tests of the injection systems. The calibrating fluid MIL-C-7024 was used as a substitute for aviation kerosene. At ambient conditions the fuel was injected into stagnant environment. Based on the measured flow characteristic and the visualization of the impinging spray it was possible to assess the dimensional quality of the fuel passages and to get an indication of the circumferential fuel homogeneity.

In a further step, detailed experimental investigations have been performed using planar non-intrusive optical measurement techniques to characterize the fuel placement, the reaction zone and the flame temperature in the primary zone of the single sector combustor (SSC) test rig up to P_{air}=13bar and T_{air}=800K. Simultaneously, conventional emission measurements were applied.

To validate the pressure dependency of the emissions and to demonstrate an acceptable operability of the lean burners at higher operating conditions, additional measurements of CO, CO_2, NO_x, O_2, UHC and soot were carried out in the HPSS rig. The water cooled combustor has a cylindrical cross section with a diameter of 90mm. The maximum operating conditions applied in this study were P_{air}=20bar and T_{air}=822K.

Based on detailed numerical and experimental results the most important design features were again "pertubated" using CFD methods. The whole development chain was repeated again with increasing refinement of the design parameters influencing the fuel-air mixing while following the optimum branch of the previous iteration.

3. Applied numerical methods

The main aim of the CFD investigations was to estimate the emission performance of different burner variants and to provide guidance for further design changes. For this study the commercially available multi-physics CFD software CFD-ACE+ [2] was used to investigate the burner performance. The code solves the gas equations in Eulerian form whereas the droplets are treated in a Lagrangian formulation with discrete trajectories. The main numerical features and physical models of the CFD code applied for the simulations are:

- block structured grids,
- finite volumes-second order spatial differencing,
- RNG k-e turbulence model with logarithmic wall functions,
- f-g mixture fraction and variance finite rate combustion model with presumed PDF,
- liquid dilute spray model with $C_{12}H_{23}$ as fuel,
- NOx production model based on oxygen equilibrium

The 3D block structured grid consists of ca. 800,000 cells representing the SSC combustor volume, the cooling passages and the burner. To enhance the improvement of the fuel injection layout more efficiently the CFD code was coupled to the optimizer package iSIGHT [3] and additional 2D calculations were performed. Within the framework of this study, a single design objective was used: lowest NOx emissions at the combustor exit. Without changing the aerodynamic shape of the injector itself, two design variables were selected: the location of the droplet break-up point after liquid sheet disintegration and the droplet velocity vector.

4. Applied experimental methods

4.1. Single Sector Combustor with optical access

The experimental facility, which was used to provide detailed information of the combustor flow field, is the Single Sector Combustor. The rig offers three-way optical access to the primary zone for application of laser light sheet techniques and is capable of operation at up to 20bars of combustor inlet pressure, 850K of air inlet temperature and preheated air mass flow rates of 1.3kg/s.

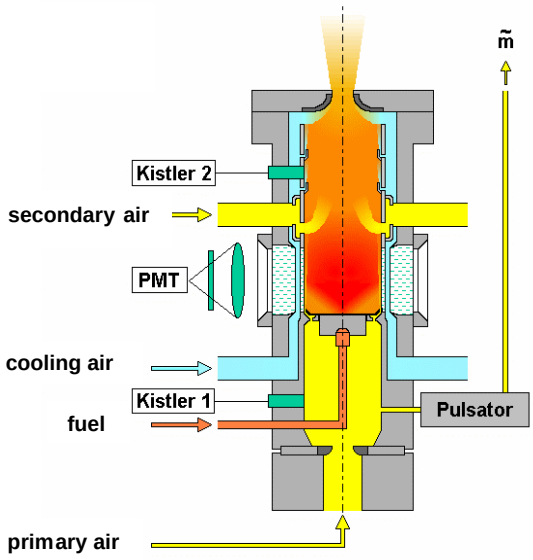

Figure 2 – Single sector combustor with optical access to the primary zone

The different flow paths for the primary air, cooling air, secondary air and the fuel supply are outlined in its schematic representation in **Figure 2**. Electrically preheated air enters the combustor plenum through a choked nozzle. It is then fed to the flame tube through the burner and the heat shield of the combustor dome plate from where it enters as a cooling and purging film along the quartz windows of the primary zone. The primary zone length is limited by addition of secondary air by means of mixing jets. The flame tube is cooled on the outside by non-preheated cooling air. All airflows exit the combustor through a single choked exit nozzle. In addition to the non-intrusive optical measurements, emission measurements in the exit of the combustor were carried out in parallel using a water cooled exhaust probe from RRD.

Table 1 gives an overview of the optical measurement techniques used for the results presented in this paper. Velocity measurements by PIV were also performed but are not presented here. For Mie-scattering the light of a pulsed, frequency doubled Nd:YAG laser was formed to a planar light sheet. The scattered light was detected perpendicular to the laser sheet by an intensified CCD camera.

Measured Quantities	**Measurement Techniques**	**Comments**
fuel distribution, liquid phase	Mie-scattering	planar, qualitative
fuel distribution gaseous and liquid	Laser-induced fluorescence of Kerosene and OH	planar, Fuel distribution qualitative, temperature quantitative
temperature		
heat release	OH*-chemiluminescence	Volumetric, quasi planar after deconvolution
fuel drop size and velocity	Phase-Doppler Anemometry	point wise

Table 1 – Summary of applied techniques

At least 150 single pulse images were taken to determine the time average of the Mie scattering. As a marker for the flame reaction zone the chemiluminescence of the OH* radical at 315±10nm was used [4] and detected by another ICCD camera. On the assumption of axial symmetry the average of 150 OH* images each having an exposure time of 10µs were deconvoluted to obtain a visualization of the reaction zone in a longitudinal section through the flame. Flame temperature is derived from the concentration of the OH radical. In lean pressurized flames the OH concentration increases nearly exponentially with temperature. By the combination of OH LIF and laser absorption measurements, absorption correction as well as absolute calibration of the OH image and therefore calculation of the spatially resolved absolute temperature becomes possible [5]. At temperatures below 1500K the OH concentration is too low for reliable temperature determination in kerosene/air flames. Despite the spectral interference of OH and kerosene LIF the simultaneous detection of the LIF signal by 2 cameras using different spectral filters enables an independent measurement of OH and kerosene. The time averaged mean and RMS values of the temperature and kerosene distribution were calculated of 200 single-pulse OH and kerosene LIF images.

For a detailed characterisation of the fuel spray, phase-Doppler anemometry (PDA) measurements were performed using a 2-component Dantec system with covariance processor. The receiving optics were positioned at Brewster's angle for kerosene (i.e. 68° off-axis), so that only light scattered by first-order refraction could be detected and the effect of changes of droplet refractive index on measured drop size was eliminated. At each node of the measurement grid covering one quarter of a cross-sectional plane of the two-phase flow, 20'000 events were recorded. A detailed account of the uncertainties of the optical measurement techniques used for spray combustion at elevated pressure is given in [6].

4.2. High Pressure Single Sector Combustor

The high pressure tests were carried out with RR's high pressure single sector combustor, which is integrated in DLR's high pressure combustor test bed 3 in Cologne depicted in **Figure 3**.

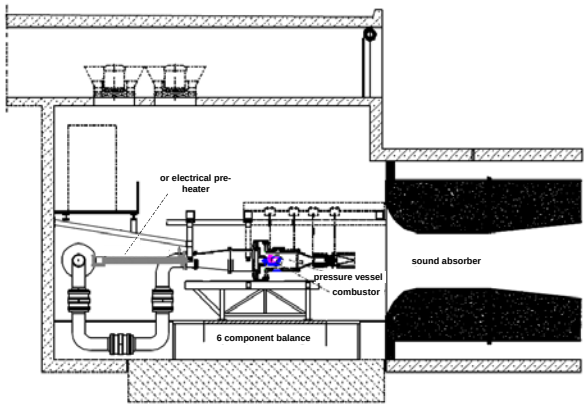

Figure 3 – DLR high pressure combustor test bed 3 with RR water cooled high pressure single sector combustor

The entry conditions realisable with the test bed are representative of modern civil aero-engines thus allowing the characterization of their emissions throughout their operating range. The high pressure sector consists of a water cooled tubular combustor with an inner diameter of 90 mm. After the constriction of the diameter at the exit, gas samples are taken via a fixed water cooled rake with 9 probe holes and averaged values for the emissions are measured by standard gas analysis equipment. The test bed is supplied with high pressure air of up to 40 bars from the central compressor station with mass and pressure controlled lines. A throttle with hydraulic control builds up the backpressure of the combustor. Two 540 KW electrical heaters supply preheat temperatures up to 920K. For higher conditions a gas fuelled non vitiated air heater can be used in a range between 800 KW and 10 MW. Kerosene is supplied through 3 separate lines with different maximum mass flows that can be controlled by pressure and mass. Pressures, temperatures and mass flows are continuously logged. Two Kistler sensors monitor the unsteady pressure in plenum and combustor thus enabling measurement of pressure oscillations in amplitude and frequency. Flashback is monitored by two flame detectors in front of the burner.

5. Burner concept

The investigated burner design is based on the so-called "swirl cup" concept. Under full load, the burner is operated at lean conditions. Two co-rotating radial air swirlers provide a high degree of swirl leading to flame stabilization close to burner exit. The fuel injection consists of two parts: a main fuel injector optimized for low emissions and a pilot fuel injector to improve flame stability and provide high combustion efficiency at part load. **Figure 4** shows a basic layout of the lean burner and a photograph of an observed flame.

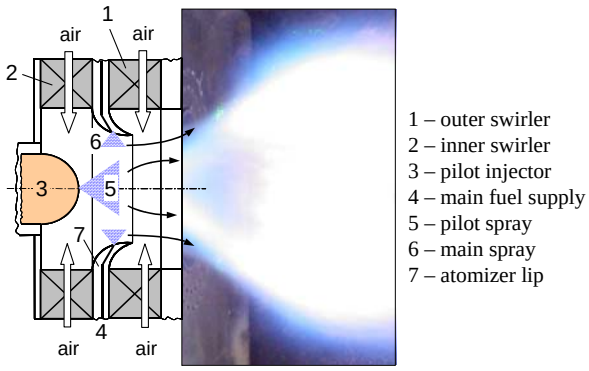

Figure 4 - Lean burner with pilot and main fuel injection, photograph of the "mixed" flame

The image was taken at a combustor pressure of 6bar, an air inlet temperature of 700K, a fuel split of 20% of the total fuel through the pilot, and a burner air-to-fuel-ration (AFR) corresponding to 92% of the design point AFR. The main fuel can be injected with discrete jets at the atomizer lip. In the present study 13 variants of multiple liquid jet injections for the main burner were investigated. Here, the number and diameter of fuel ports as well as the circumferential injection angle of the fuel jets were varied. Three alternative burner variants were investigated additionally e.g. one with a prefilmer.

6. Results – development phase I

6.1. Numerical investigations

Initial CFD calculations were performed to optimise the fuel injection with respect to NOx emissions without changing the aerodynamic shape of the burner. The fuel injection position was varied between the lower surface of the filmer lip corresponding to r=0% and the tip of the central fuel injector at r=100%. **Figure 5** shows a schematic of the investigated numerical domain inside the burner.

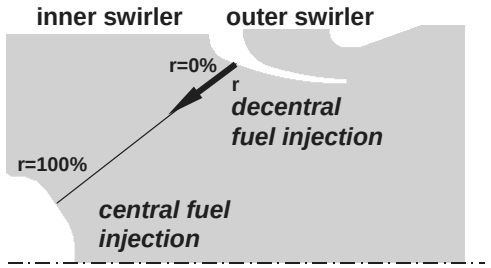

Figure 5 – Schematic of investigated fuel release points inside the lean burner

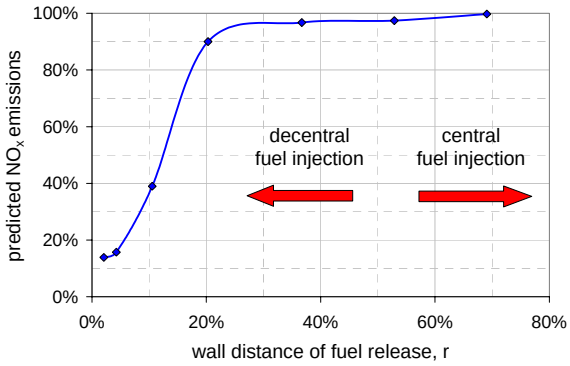

Figure 6 – Predicted NOx emissions vs. fuel injection release point r inside the burner, P_{air}=20bar, T_{air}=822K

The results are given in **Figure 6**. Here, NOx emissions are normalized with the value at r=100%. Above r=40% r has only a minor effect on NOx emissions. However when shifting from a central (r>70%) to a decentral mode (r<30%), NOx emissions decrease nearly exponentially with r. If r is close to 0, a NOx reduction of up to 85% compared to central injection was predicted. The predicted temperature distributions for the central and decentral fuel injection is given in **Figure 7**.

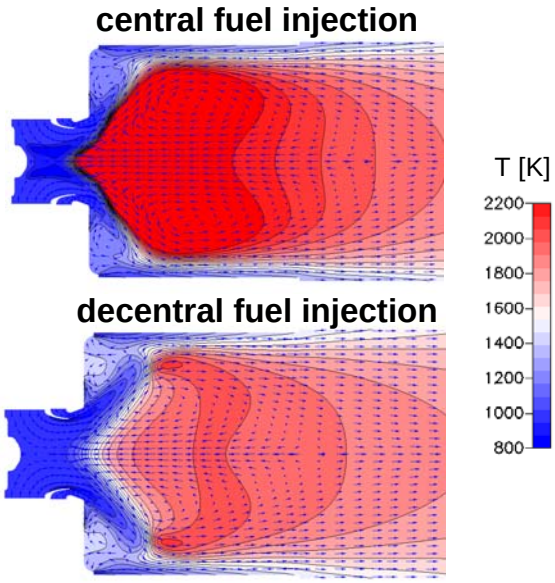

Figure 7 – Predicted temperature distribution, central and decentral fuel injection, P_{air}=20bar, T_{air}=822K

With central injection the flame is attached to the burner exit. A high proportion of unevaporated droplets is recirculated on the burner axis. This results in significant heat release. With r<30% the liquid fuel is injected in regions with high flow velocities. This case burns in a detached mode with a certain lift-off distance exhibiting better temperature homogeneity and lower peak temperatures.

6.2. Derived burner design, kit of parts

Based on the results of the areforementioned CFD investigations and assuming a constant fuel flow number, 3 burner variants were designed.

Figure 8 shows a schematic of the “kit of parts” for the phase I fuel injector.

Within the study two different module sizes with effective areas of A_{eff}=420mm^2 (burner IA) and A_{eff}=720mm^2 (burner I-B) were investigated.

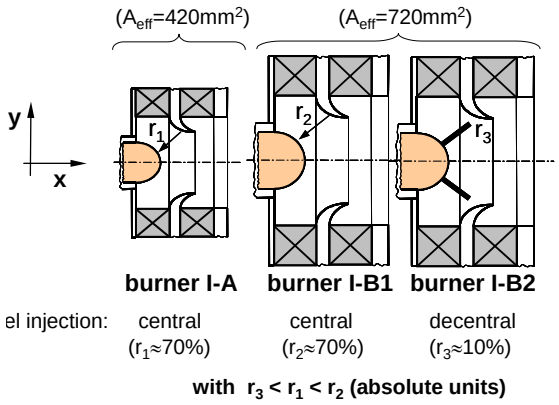

Figure 8 – Schematic of investigated burner variants for development phase I, variation of the fuel release point r

For burner I-B two fuel release points at r_3=10% and r_2=70% were designed. Due to the reduced module size of burner I-A, burner I-B1 has the highest wall distance for the fuel release point.

6.3. Experimental results

The emissions of CO, CO_2, NO_x, O_2, UHC and soot of the phase I burners were measured in the HPSS combustor. The main conditions were at P_{air}=6bar, T_{air}=780K and P_{air}=20bar, T_{air}=822K. **Figure 9** shows a variation of $EINO_x$ over burner AFR for configuration I-B1 and -2. The emissions are normalized with the I-B1 emission at 80% nominal AFR. The curves exhibit the expected nonlinear rise towards richer conditions, which is more pronounced for the decentral injection of I-B2 indicating the higher homogeneity of its mixture. The reduction against I-B1 at 100% burner AFR is 65%.

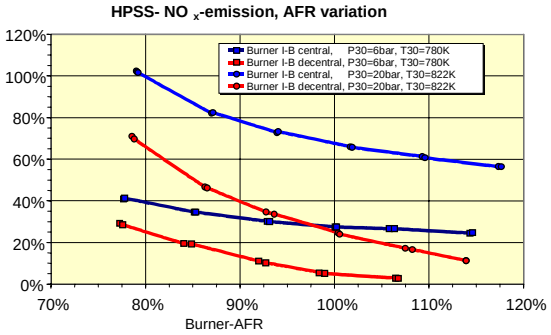

Figure 9 – Measured EINOx over nominal burner AFR normalized at 80% AFR for burner I-B1, –2

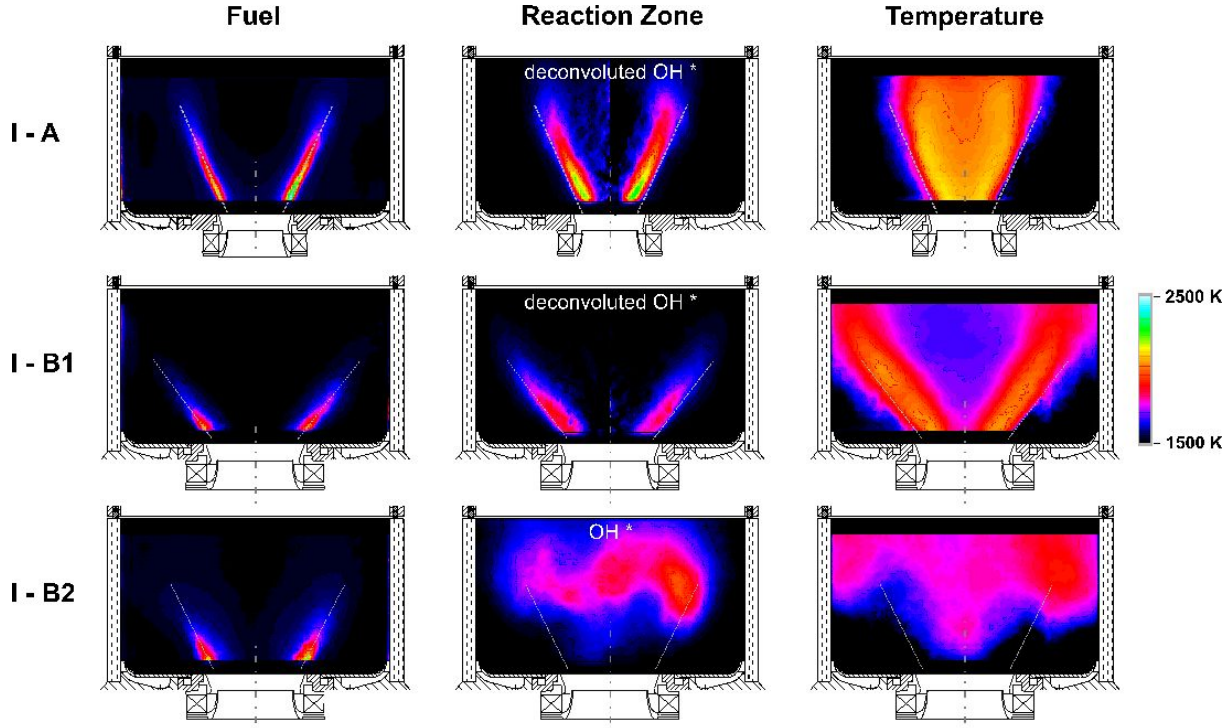

Figure 10 – Comparison of: on the left column fuel distribution imaged by LIF of Kerosene, in the middle OH* chemiluminescence and on the right temperature measured on the OH-LIF signal for 3 development phase I burners at P_{air}= 6bar and T_{air}=700K preheat. The images are averaged over 200 single shots.

A rather similar decrease of NO_x between I-B1 and -2 burner in calculation and measurement in HPSS was obtained. Although this already could be taken as endorsement of the CFD optimisation procedure, detailed measurements for the 3 phase I configurations at up to 13bar were made in the SSC combustor in a next validation step. The relation between fuel placement, heat release and temperature homogeneity was to be acquired to gain understanding of the link between geometrical variation and resulting emission. **Figure 10** reflects an exemplary result for one typical operating condition.

The Kerosene LIF shows the contributions from the liquid and gaseous phase and gives therefore a qualitative picture of fuel consumption. For the smaller burner I-A with central injection, the expansion angle of the fuel distribution is small. The flame as represented by the deconvoluted OH* signal burns as a diffusion flame at the inner rim of the fuel cone with high intensity near the burner mouth, resulting consequently in rather high temperatures at the inner edge of the heat release zone.

For the larger burner I-B1, the expansion angle of fuel cone is wider and the fuel is consumed earlier. The radial width of the fuel distribution is increased and with a higher radial position this leads to higher dilution and less intensive heat release as observed by comparison of the two deconvoluted OH* images. The peak temperatures are lower, but the recirculation zone on the axis is rather cold. However the flame and the liquid sheet can be easily observed by eye from an elevation angle of 45°, permitting a look into the burner showing a stabilisation of the flame in the swirl cup for both burners. Based on the results of a recent isothermal investigation of liquid sheets in swirling flow [7], it can be assumed, that the swirl in the inner cup is too weak to transport the fuel to the filmer lip and is instead transported towards the upstream extension of the recirculation finding favourable conditions for ignition.

Burner I-B2 on the other hand clearly exhibits a lifted flame as seen from the OH picture. Here the radial symmetry was not sufficient to deconvolute the image. The radial dispersion of the fuel is even wider here and together with the lift-off length of the flame almost complete prevaporization and good premixing is achieved, which yields a quite homogeneous temperature field with low combustion temperatures.

7. Results – development phase II and III

7.1. Numerical investigations

Based on the promising low NO_x emissions measured for the decentral fuel injection of burner I-B2, the evelopment chain was repeated twice. Detailed CFD simulations were carried out to investigate the effect of fuel jet penetration into the central recirculation zone on flame position and NO_x emissions. As an example, the effects of varying fuel flow number and circumferential fuel swirling were analysed. **Figure 11** demonstrates the advantageous effect of an increased number of fuel ports on peak temperature reduction and improved temperature homogeneity. For all cases, the flame location is nearly unaffected.

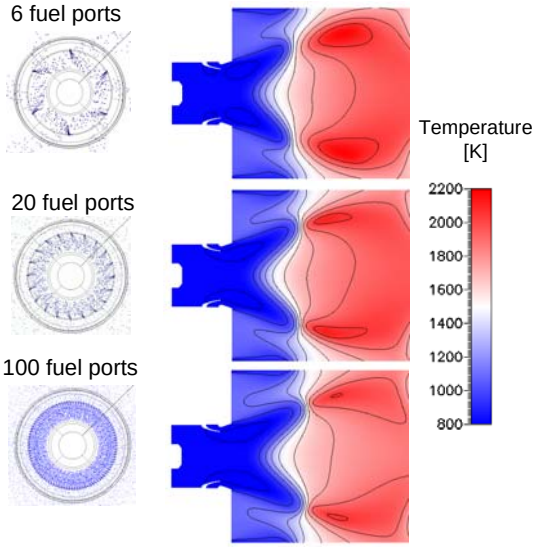

Figure 11 – Predicted temperature distribution, influence of initial fuel homogeneity, main fuel injection only, P_{air}=20bar, T_{air}=822K

Additionally, it was demonstrated that the positive effect of limited fuel jet penetration can be augmented by circumferential swirling of the fuel jets (**Figure 12**). Compared to orthogonal fuel injection, co-swirl of fuel and air reduces the number of droplets evaporating in the central recirculation. As a result of a reduced fuel penetration in flow regions with high turbulent shear stresses, calculated NO_x emissions were reduced up to 54%. Applying a counter swirl of fuel and air, NOx can again deteriorate by 15% compared to orthogonal injection.

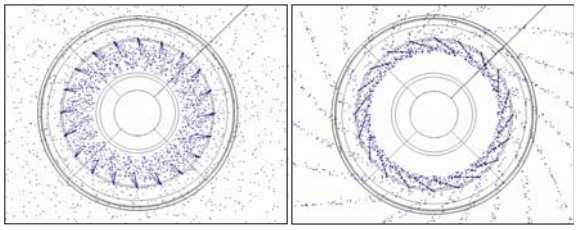

Figure 12 – Illustration of orthogonal and swirled fuel injection at the atomizer lip (looking downstream)

Further numerical simulations were carried out using optimiser strategies to identify alternative fuel injections methods allowing a limitation of the penetration of fuel towards the central recirculation zone.

7.2. Derived burner design, kit of parts

Figure 13 summarizes the investigated fuel injection concepts for the lean burner within this study. As a result of a high combustion stability observed for burners I-A and I-B1 with central fuel injection all injectors of phase II and III the same pressure swirl atomizer was used as a pilot stage to stabilise the flame.

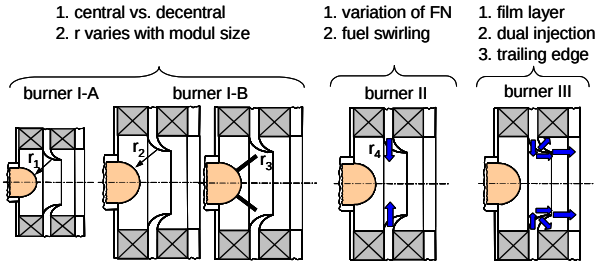

Figure 13 – schematic of investigated fuel injection concepts, development phases I to III.

For the development phase II a kit of parts with 6 injection variants was manufactured. The investigation was focused on the effect of varying burner fuel flow numbers for the main stage on fuel-air mixing. The number of injection holes and hole diameter was therefore changed accordingly with a lower and higher value for each parameter. In addition a variant with fuel holes inclined in the air swirl direction was derived. In a further phase III, 6 more burner variants were designed. Based on the successful concept of fuel swirling for the main stage leading to a limited penetration of the fuel towards the burner centerline, the following variants were investigated: fuel injection in inner and outer air stream, prefilmer, swirled fuel injection through the trailing edge of the filmer lip, multiple spray injection. Especially for the trailing edge injection CFD results have shown a NOx reduction up to 10% compared to the best configuration with swirled fuel injection of phase II.

7.3. Experimental results

7.3.1 Development phase II

All HPSS tests of phase II and III were done with 10% of the fuel going through the central pilot. The emission measurements on the HPSS showed, that variations with the same momentum ratio of fuel jet to gas flow, and thus fuel penetration exhibited very similar results. The variant with an initial momentum in swirl direction had the lowest emissions at high pressure with a 68% reduction against the

central injection. This result was even better than the fuel placement device of burner I-B2.

At the SSC, a slightly different sample was investigated to get insight into the remaining burner variants: beside the successful swirl version an injection with mean and high flow number and thus lower jet momentum. However the comparison of Mie scattering and Kerosene LIF on one side and the OH* emission and OH-LIF based temperatures on the other side showed, that for the medium conditions of 6bar and 700K or 822K tested here, the distributions were rather similar. That points to a pressure dependence of the penetration and early mixing, which is not described by jet to cross flow momentum ratio alone. More detailed investigations are needed to understand the mixing behaviour of fuel jets in swirling flow with streamline curvature.

PDA measurements were carried out for the swirled version at an axial distance of 8mm behind the burner exit. For that position, approximately the inner half of the fuel distribution was within the high temperature region. Consequently measured SMD's were higher in this region, whereas at the outer side, where the number of small droplets is relatively unaffected from flame induced evaporation the SMD's measured at different angular positions were below 18µm.

7.3.2 Development phase III

For the HPSS measurements at 6bars a spread of the resulting NOx emissions over burner AFR was observed. The injection into inner and outer swirl passage was worse than the central injection baseline case at rich conditions leading to the assumption that stoichiometric burning zones are stabilized downstream of the outer swirl channel. The trailing edge injection is similar as the phase II burners, whereas the swirling injection has the best results with little differences for the higher number of holes, showing that an optimum circumferential homogeneity can be reached with a medium number of jets. At 20bars, the spread of NOx emission curves is considerably reduced, with the trailing edge injection giving the best result, comparable with the high flow number swirled injection of the best configuration of the phase II injector.

Three off the six phase III burners were investigated on the SSC: swirled injection (config. A), prefilmer (config. C) and trailing edge injection (config. E). For a variation of fuel splits between pilot and main between 0% and 100%, gas analysis was performed at 6bar and 700K as well as 822K preheat (**Figure 14**). In the low power region the prefilmer with near zero fuel momentum burns most stable and has the lowest emission of both species followed by the swirl injection at trailing edge and filmer lip. At 700K the trailing edge injection produces nearly the same NOx emissions as the prefilmer. It has to be mentioned that the 822K condition reflects a pressure scaled full power case at which the pilot stage is operated with a fuel fraction of ca. 10%.

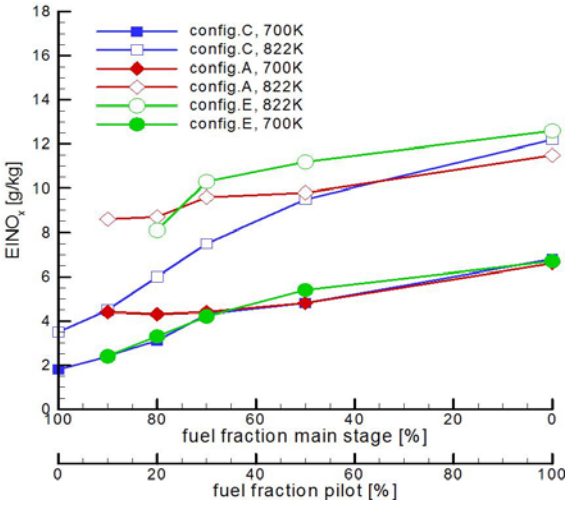

Figure 14 – NO_x emissions measured in SSC at 6bars and 700K resp. 822K, AFR= 0.92 AFR_{design} for config. A, C and E (phase III)

For the prefilming burner, operation was even possible without pilot. It shows a lifted flame that does not recirculate hot products in the central recirculation zone. For pilot operation of 20%, the OH-temperature single shot images in **Figure 15** shows continuous high temperature zones.

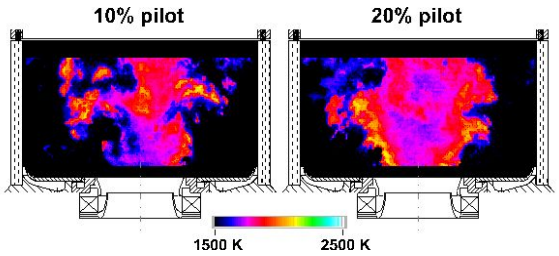

Figure 15 – OH-LIF based single shot temperature at 6 bars and 700 K for config. C of phase III at AFR=0.92 AFR_{design}

From 20 to 30% pilot fuel, the expansion angle of the heat release zone widens considerably, such that the flame eventually fills out most of the combustor cross section as can be seen by comparing the pictures in the right column of **Figure 16**. At the same time the fuel evaporation as shown by Kerosene-LIF is faster. The maximum heat release is still locally separated emerging only after most of the fuel has vanished and is detached from the heat release zone of the pilot. This is coincident with the rapid reduction of CO emissions to a level that doesn't significantly change for higher pilot fuel. With an even split of pilot and main fuel, rapid heat release begins right at the burner outlet, the pilot fuel burning in diffusion mode.

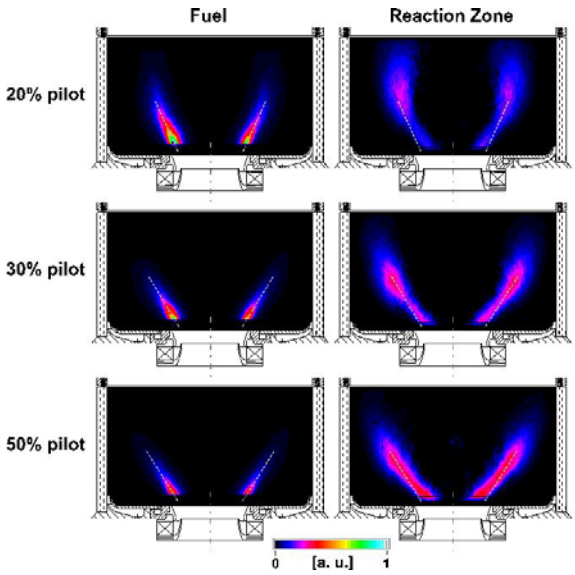

Figure 16 – Mean Kerosene-LIF and deconvoluted OH* distributions for config. C of phase III at 6bars and 700K, AFR=0.92 AFR_{design} at varying degrees of pilot fuel injection

These observations suggest some conclusions concerning the role of an optimum pilot operation: When a stable pilot-reaction sheet is produced, overall stability does not depend on the main burner. Therefore, a main burner producing a fuel placement at a high radial position and a long flame liftoff, thus having the best premixing will give the best NO_x results. The flow field needs to ensure that the flame spreads radially outward quick enough to ensure full oxidation of the fuel in the primary zone for good combustion efficiency. The pilot combustion must produce enough heat convection to ensure stable main fuel combustion but should be limited to keep the main heat release at a distance from the burner allowing enough premixing. Since this is a crucial balance, the fuel split must be made adjustable to fit the thermodynamics produced by the respective operating conditions.

8. Discussion and conclusions

The applied development chain has been used to generate validated design rules for low NOx fuel injection systems. Based on the initial burner design the fuel injector was continuously refined in 3 steps. The main results can be summarized as follows:

Lowest NOx emissions are observed with main burners offering a low fuel penetration into the central recirculation zone at the burner axis. Since the velocity gradients perpendicular to the atomizer lip are very high, changing the jet momentum has a twofold effect: A difference in fuel penetration will have a significant influence on its radial dispersion, if the fuel is able to follow diverging streamlines entering the combustor. This ability depends on drop size, which is mostly influenced by the magnitude of the relative velocity to the gas flow during the atomization process. Since the conversion from jet to ligaments and droplets happens in a distance from the orifice where most of the jet momentum is consumed, c.f. [8] the local velocity there decides the droplet diameter. For the highly swirling flow field inside the swirl cup, the axial velocity increases from centre to wall with a high velocity region

near the wall. Hence the liquid should not leave this zone to achieve good atomization. A fuel placement in a high velocity zone will furthermore assure a good dilution of the spray in the direction of the streamlines during the acceleration phase and enable secondary atomization if the fuel can be kept in the high velocity region long enough.

In this configuration a fuel placement as near as possible to the streamline separating inner and outer air swirl leads to a significant radial transport of the fuel, thereby achieving further dilution of the spray and, the piloted flame penetrating with an angle radially outward, a longer liftoff length of the flame allowing more time to premix and prevaporize. The measured SMD of 18µm is small enough to achieve prevaporized combustion of the main fuel at the highest flame liftoff observed, cf. **Figure 16**.

A swirled fuel injection and an increased fuel flow number via increased port diameters reducing the jet momentum perpendicular to the atomizer lip have consequently shown a significant NOx reduction of ca. 68% compared to central fuel injection. A trailing edge injection of the main fuel with no premixing of the main fuel and air within the burner has demonstrated lowest NOx emissions in the lean regimes at higher operating conditions up to 20bar.

As shown for the prefilmer concept (c) of phase III, the fuel split has a significant effect on the flame structure, the location of the reaction zone, and the evaporation behaviour of the "mixed" flame. Consequently, the NOx emissions increase strongly with higher fuel splits. At the same time, the flame position changes from a lifted flame to an anchored flame with increased spray angle.

Finally, to improve the fuel injection system towards a production standard application and with the use of design rules from the described development chain further validation steps have to be carried out e.g. full-annular testing.

9. Acknowledgements

This work has been funded by the German Federal Department of Economy and Labour under contract no. 0327090B (RRD) and no. 0327090E (DLR) within the AG Turbo collaborative program "500 MW on a single shaft". The support is gratefully acknowledged. Additionally, special thanks are expressed for the excellent support from ANECOM Aerotest GmbH during the HPSS test campaign and to the work of J. Becker, W. Quade on the SSC.

10. Literature

[1] Bake, S., Gerendas, M., Lazik, W., Dörr, Th., Schilling, Th.: *Entwicklung eines Magerverbrennungskonzeptes zur Schadstoffreduzierung im Rahmen des nationalen Luftfahrtforschungsprogramms ENGINE 3E*, DGLR-2004-182.

[2] CFDRC Research Corporation, 2004, *CFD-ACE+ Users Manual*.

[3] Engineous Software, 2004, *iSIGHT Vers. 8.01. User Manual*.

[4] Najim, H.N., Paul, P.H., Mueller, C.J., Woyckoff, P.S.: *On the adequacy of certain experimental observables as measurements of flame burning rate*, Combustion and Flame, **113**, pp. 312-322, 1998.

[5] Behrendt, Th., Heinze, J., Hassa, C.: *Experimental investigation of a new LPP injector concept for aero engines at elevated pressures*, Proceedings ASME GT2003-38444, pp. 1-10, 2003.

[6] Behrendt, Th., Heinze, J., Hassa, C.: *Optical Measurements of the Reacting Two-Phase Flow in a Realistic Gas Turbine Combustor at Elevated Pressures*, ILASS-Europe, 2000

[7] Becker, J. and Hassa, C.: *Experimental Investigation of Spatial and Temporal Aspects of the Liquid Fuel Placement in a Swirl Cup at Elevated Pressure*, ASME GT2004-53524, pp 1-10, 2004.

[8] Becker, J. and Hassa, C.: *Breakup and atomization of a kerosene jet in crossflow at elevated pressure*, Atomization and Sprays, vol. 11, pp.49-67, 2002.